

Effect of Iron Ore Tailings Replacing Porous Basalt on Properties of Cement Stabilized Macadam

Qifang Ren¹, Fan Bu¹, Qinglin Huang¹, Haijun Yin², Yuelei Zhu¹, Rui Ma¹, Yi Ding¹, Libing Zhang³, Jingchun Li³, Lin Ju³, Yanyan Wang⁴, Wei Xu⁵, Haixia Ji¹, and Won-Chun Oh^{6†}

¹School of Materials Science and Chemical Engineering, Anhui Jianzhu University, Hefei 230601, China

²Beijing Rechsand Sand Industry Casting Material Co., Ltd., Beijing 100005, China

³Anhui Road and Bridge Engineering Group Co., Ltd., Hefei 230088, China

⁴Anhui Institute of Building Research and Design, Hefei 230031, China

⁵Anhui Construction & Building Materials Technology Group Co., Ltd., Hefei 230001, China

⁶Department of Advanced Materials Science and Engineering, Hanseo University, Seosan 31962, Republic of Korea

(Received January 22, 2024 : Revised June 7, 2024 : Accepted June 7, 2024)

Abstract In this paper, iron ore tailings (IOT) were separated from the tailings field and used to prepare cement stabilized macadam (CSM) with porous basalt aggregate. First, the basic properties of the raw materials were studied. Porous basalt was replaced by IOT at ratios of 0, 20 %, 40 %, 60 %, 80 %, and 100 % as fine aggregate to prepare CSM, and the effects of different cement dosage (4 %, 5 %, 6 %) on CSM performance were also investigated. CSM's durability and mechanical performance with ages of 7 d, 28 d, and 90 d were studied with the unconfined compression strength test, splitting tensile strength test, compressive modulus test and freeze-thaw test, respectively. The changes in Ca²⁺ content in CSM of different ages and different IOT ratios were analyzed by the ethylene diamine tetraacetic acid (EDTA) titration method, and the micro-morphology of CSM with different ages and different IOT replaced ratio were observed by scanning electron microscopy (SEM). It was found that with the same cement dosage, the strengths of the IOT-replaced CSM were weaker than that of the porous basalt aggregate at early stage, and the strength was highest at the replaced ratio of 60 %. With a cement dosage of 4 %, the unconfined compressive strength of CSM without IOT was increased by 6.78 % at ages from 28 d to 90 d, while the splitting tensile strength increased by 7.89 %. However, once the IOT replaced ratio reached 100 %, the values increased by about 76.24 % and 17.78 %, which was better than 0 % IOT. The CSM-IOT performed better than the porous basalt CSM at 90 d age. This means IOT can replace porous basalt fine aggregate as a pavement base.

Key words cement stabilized crushed stone material, iron ore tailings, porous basalt, mechanical properties.

1. Introduction

At present, semi-rigid base occupied a large proportion in road engineering, and cement stabilized macadam (CSM) was widely used as a semi-rigid material.¹⁻³⁾ The aggregate commonly used in CSM were limestone, granite and so on,^{4,5)} which has higher strength and smaller crushing index. However, because of the short of natural aggregate, especially the high quality stones, more renewable materials were

necessary to decline the environment impact and construction cost. In the construction of road base, solid waste can be used to partially replace natural raw materials to offset the lack of raw material and improve the storage problems for massive amount of solid waste.⁶⁻⁹⁾

Iron ore tailings (IOT) is a waste generated from the extraction of industrial ores.^{10,11)} According to relevant reports, 1 ton of fine iron ore produced 2.5 to 3 tons of tailing. So IOT has become one of the largest solid wastes in terms of pro-

[†]Corresponding author

E-Mail : wc_oh@hanseo.ac.kr (W.-C. Oh, Hanseo Univ.)

© Materials Research Society of Korea, All rights reserved.

This is an Open-Access article distributed under the terms of the Creative Commons Attribution Non-Commercial License (<http://creativecommons.org/licenses/by-nc/3.0>) which permits unrestricted non-commercial use, distribution, and reproduction in any medium, provided the original work is properly cited.

duction and storage. More and more IOT are being created, with an increasing of accumulation volume, but the comprehensive utilization efficiency is low, which caused growing serious environmental pollution problems. In order to achieve sustainable development of waste, a large number of IOT was utilized in engineering to increase the recycled application.^{12,13)} In recent years, many researchers used discarded IOT to produce concrete and other building materials.¹⁴⁻¹⁶⁾ IOT was used as cementitious material in concrete,^{17,18)} and the effects of IOT and fibers on the performance of concrete were studied,¹⁹⁾ there were also researches about IOT used in steam concrete research.^{20,21)} To investigate the effect of IOT on building material technology, Fontes et al.²²⁾ formulated three mixtures: conventional mortar, mortar with IOT completely replaced natural aggregate, and mortar with IOT replaced lime, with the replacement ratio ranged from 10 % to 100 %. The bulk density and water demand ratio were increased in IOT slurry has increased, and mechanical properties were improved. IOT could also use as fine aggregate to substitute natural or artificial sand to prepare IOT concrete.²³⁻²⁵⁾ Abd Latif et al.²⁶⁾ prepared concrete using tailings and sand with different proportions, and found that with the raised ratio of tailings, the density and permeability of the concrete were increased. In order to reduce the cost of concrete construction, Zhao et al.²⁷⁾ used IOT instead of natural aggregate to prepare ultra-high performance concrete (UHPC) under two different curing regimes. It was found that the workability and compressive strength of UHPC was sharply decreased with 100 % replaced ratio, and the pores in UHPC became coarse if more IOT was added.

In the road construction, the CSM base has the advantages of high strength and good integrity.²⁸⁻³⁰⁾ Solid waste is also widely used in pavement base.^{31,32)} Some researchers use recycled aggregate instead of natural aggregate for pavement base, Zhang et al.³³⁾ prepared CSM with recycled aggregate for pavement base, and found that when the cement content was 4 %, it matched the requirements of domestic expressway and primary highway base. Lan et al.³⁴⁾ study the influ-

ence of mechanical properties and shrinkage properties CSM using 0~2.36 mm reclaimed fine aggregate (RFA) to replace natural aggregate. The results shown that unconfined compressive strength (UCS) and indirect tensile strength (ITS) were affected by different dosage of cement. For open grade cement stabilizing material (OGCSM), Yan et al.³⁵⁾ prepared OGCSM with recycled aggregate, and proved that OGCSM was preferred to be applied on expressway base layer with 0~100 % recycled aggregate instead of natural aggregate. Yan et al.³⁶⁾ also used solid waste incineration (SWI) bottom ash (BA) as a cement-stabilized macadam material. Reuse of industrial waste or construction by-products, including dredged river sediment (DRS), IOT slag (ITS) and calcium carbide slag (CCS), in the production of building materials decreased construction costs, reduced storage requirements and protected the environment. Chu et al.³⁷⁾ used waste (DRS, ITS and CCS) as backfill materials in mined-out areas. Bastos et al.³⁸⁾ used IOT as road engineering materials and found that waste could be used in road engineering. On the whole, the application of IOT in pavement grassroots was relatively rare, but CSM was still used in grassroots research.

In this paper, IOT used to replace porous basalt fine aggregate with different ratio (0, 20 %, 40 %, 60 %, 80 %, 100 %) to prepare CSM, and the mechanical and durability properties were studied. The influence of IOT replacement ratio on CSM performance was analyzed from a macro perspective. Cement dosage of 4 %, 5 %, and 6 % were respectively used to study the influence of different cement dosage on CSM performance.

2. Experimental Procedure

2.1. Material of experiment

The cement used in this project was P.O 42.5 cement produced by Anhui Conch Company, and its main properties are shown in Table 1. The porous basalt used in this research was produced in Chuzhou, Anhui Province, and was divided into three types based on the Chinese standard JTG/T.F20-2015

Table 1. Physical properties of P.O 42.5 cement.

Project	Volume stability	Setting time (min)		Compressive strength (MPa)		Rupture strength (MPa)	
		Initial set	Final set	3 d	28 d	3 d	28 d
Index	Qualified	156	215	26.9	47.1	5.6	8.2

suggested particle size range, which was 0~4.75 mm, 4.75~9.5 mm, and 9.5~19.5 mm, in that order. IOT was iron tailing ore debris with a particle size of 0~4.75 mm from Anhui Province. The water absorption and water content are listed in Table 2. The microtopography of IOT is shown in Fig. 1, the surface shows a granular structure, which is relatively rough and has a large number of crystal angles. The chemical composition of IOT by X-ray fluorescence (XRF) is shown in Table 3, the main elements in IOT are Si, Al, Fe and Ca.

Table 2. Technical parameters of the aggregate.

Aggregate particle size (mm)	Apparent density (g/cm^3)	Water absorption rate (%)	Crushing value (%)
9.5~19	2.532	3.097	28.927
4.75~9.5	2.647	5.061	-
0~4.75	2.716	7.232	-
0~4.75 (IOT)	2.821	9.924	-

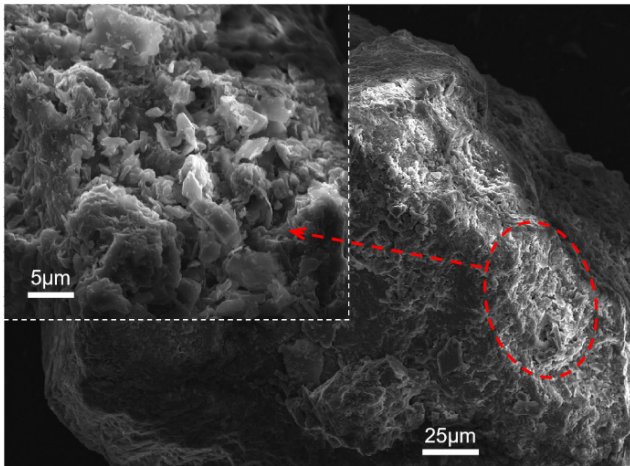


Fig. 1. Micro-morphology of IOT.

Table 3. Chemical composition of IOT (%).

Na ₂ O	MgO	Al ₂ O ₃	SiO ₂	P ₂ O ₅	SO ₃	Cl	K ₂ O	CaO	Fe ₂ O ₃
4.853	5.037	16.552	42.811	3.071	4.155	0.073	1.368	8.422	12.678

Table 4. Test scheme of mechanical properties of cement stabilized IOT mixture.

Mechanical performance index	The content of IOT (%)	Cement dosage (%)
Unconfined compressive strength	0, 20, 40, 60, 80, 100	4, 5, 6
Splitting strength	0, 20, 40, 60, 80, 100	4, 5, 6
Compressive rebound modulus	0, 20, 40, 60, 80, 100	4, 5, 6
Freeze-thaw test	0, 20, 40, 60, 80, 100	4, 5, 6

2.2. Compaction test and mix proportion

In this experiment, the laboratorial impact test for aggregates were using a standard cylinder to instead the field roller in construction site. According to the standard test method of “Test Methods of Materials Stabilized with Inorganic Binders for Highway Engineering” (JTGE51-2009),³⁹⁾ the type B compaction method was selected for compacted stabilization of gravel. The mixture specimens were weighed according to designate proportions, and mixed until uniform. The mixed material was divided into three groups, and each group was filled into the test cylinders respectively with three hammering layers, beaten 59 times each layer. After the sample was formed, the substrate and the liner were removed, the outer wall of the striking cylinder was wiped to weight. Finally, the sample in the cylinder was pushed out by the demold machine.

In this paper, porous basalt aggregate, IOT and P.O42.5 cement were mainly used to prepare CSM. The cement ratio of 4 %, 5 %, and 6 %, as well as the IOT substituted ratio of 0 %, 20 %, 40 %, 60 %, 80 %, and 100 % were applied to study the influence of different materials content. The experiment scheme is shown in Table 4. The grading curve of the control group is shown in Fig. 2, which meets the dense distribution range (JTGT.F20-2015).⁴⁰⁾ The variation curves of maximum dry density and optimal moisture content are shown in Fig. 3. It can be seen from the figure that with the increase of cement dosage, the maximum dry density of CSM was increased and the optimal moisture content was decreased. When the cement dosage was fixed, the maximum dry density of CSM was gradually decreased and the optimal moisture content was increased with the increase of IOT content.

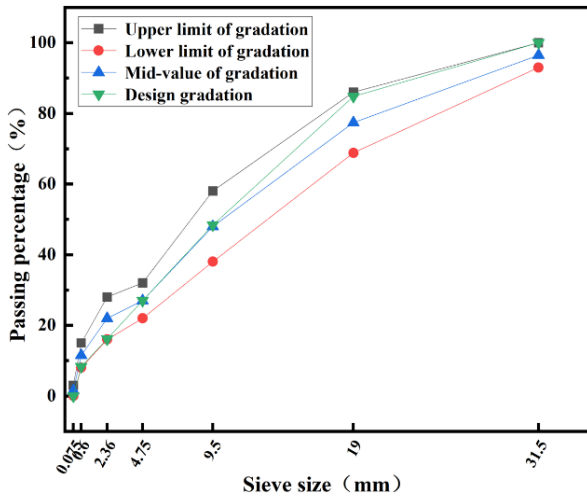


Fig. 2. Particle size gradation of cement stabilizing materials with IOT.

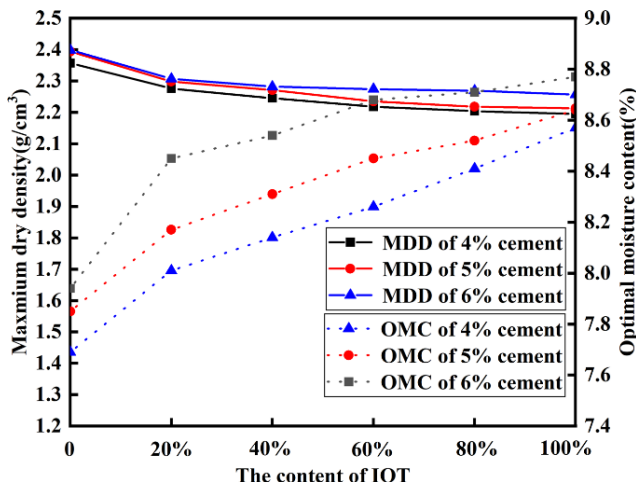


Fig. 3. Results of the compaction test of IOT (%) for different cement dosages (left axis: MDD; right axis: OMC).

2.3. Testing method

The test sample was prepared according to the optimum water content and maximum dry density of cement stabilized crushed stone above test. The used aggregate was determined according to the screening test results of main aggregates.

According to standard of test method of “Test Methods of Materials Stabilized with Inorganic Binders for Highway Engineering” (JTGE51-2009),³⁹⁾ the size of the mold was 100 mm in diameter and height. The mechanical properties were tested by YAW-2000 microcomputer controlled pressure testing machine produced by Shanghai Sinisheng Machinery Manufacturing Co., Ltd. The loading speed was set at 1 mm/min. Finally, the prepared specimens which cured for 7 d, 28 d, and 90 d were tested. In freezing-thawing test, 150 mm × 150 mm cylinder specimens were used. According to test procedures for “Test Methods of Materials Stabilized with Inorganic Binders for Highway Engineering” (JTGE51-2009),³⁹⁾ the specimens were freezing-thawing for 5 cycles and kept in standard condition for 28 d. Finally, BDR (loss rate of compressive strength of freezing-thawing specimens) of CSM were calculated.

Ethylene diamine tetraacetic acid (EDTA) titration method, which was designed on the basis of the specification of test rules for “Test Methods of Materials Stabilized with Inorganic Binders for Highway Engineering” (JTGE51-2009).³⁹⁾ As shown in Fig. 4, the calcium ion was titrated with EDTA-2Na, and the color in the mixture was firstly changed from rose red to purple and finally to dark blue. The end point of the complexation reaction of Ca²⁺ can be determined by the gradual addition of EDTA-2Na solution, where a change in color can be observed. EDTA-2Na binds to Ca²⁺ eventually forming a dark blue complex. The dosage of consumption of EDTA-2Na was recorded. Finally, scanning electron microscopy (SEM) was used to observe the microstructure of CSM-IOT at different curing ages.

3. Results and Discussion

3.1. Unconfined compressive strength

As seen in Fig. 5 is CSM-IOT with varied cement dosage



Fig. 4. Diagram of changes in titration process.

of 4 %, 5 %, and 6 %, respectively. It could be found that with the increase of cement, the unconfined compressive strength of the mixture was also increased, and the unconfined compressive strength was increased with the growth of curing age. At 7 d, the strength of the mixture with a IOT replaced ratio of 0 % was the highest. The strength value was 4.2 MPa. When the replaced ratio reached 100 %, the strength was the lowest with the value of 3 MPa. The results indicated that the incorporation of IOT led to the reduction of the early strength of the mixture. With the increase of curing age, at 28 d, with the same dosage of cement, the strength with the replaced ratio of 60 % was the highest, which increased about 38.29 %.

The particle size of IOT was finer than that of porous basalt sand, it was better filled the inter voids of the mixture. However, when the amount of IOT was too much, it affected the overall strength of the mixture. IOT itself has more defects and its own strength is low, so that the strength of 60 % was the best. Because the cement was mostly completed hydration reaction at this time. SiO_2 , Al_2O_3 and other volcanic materials in IOT was reacted with $\text{Ca}(\text{OH})_2$ from cement hydration, and the reaction rate was relatively fast.

Therefore, the strength of some mixtures replaced by IOT was exceeded the replacement rate of 0. When the curing age was 90 d, the maximum growth rate of 100 % IOT content was 31.84 %. When the IOT replaced ratio was 0, the growth rate was only 11.05 %, which means that the volcanic ash reaction inside the IOT-CSM I was more intense, so the overall strength of the mixture increased with the increase of the IOT replaced ratio. When the cement dose was 6 %, the 90 d compressive strength with a 100 % IOT replacement ratio was 7.12 MPa.

3.2. Splitting strength

As shown in Fig. 6 is splitting strength of CSM-IOT with 4 %, 5 %, and 6 % cement dosage, respectively. The splitting strength was increased with the increase of cement dosage. As shown in Fig. 6(a), when the curing age was 7 d, the maximum splitting strength of CSM with IOT replaced ratio of 0 % was 0.32 MPa, while the minimum splitting strength of CSM with IOT content of 100 % was 0.26 MPa. At the early age, the strength of CSM with IOT replaced ratio of 0 % grew faster, while the strength of IOT cement stabilized macadam grew slower. With the increase of curing age, the

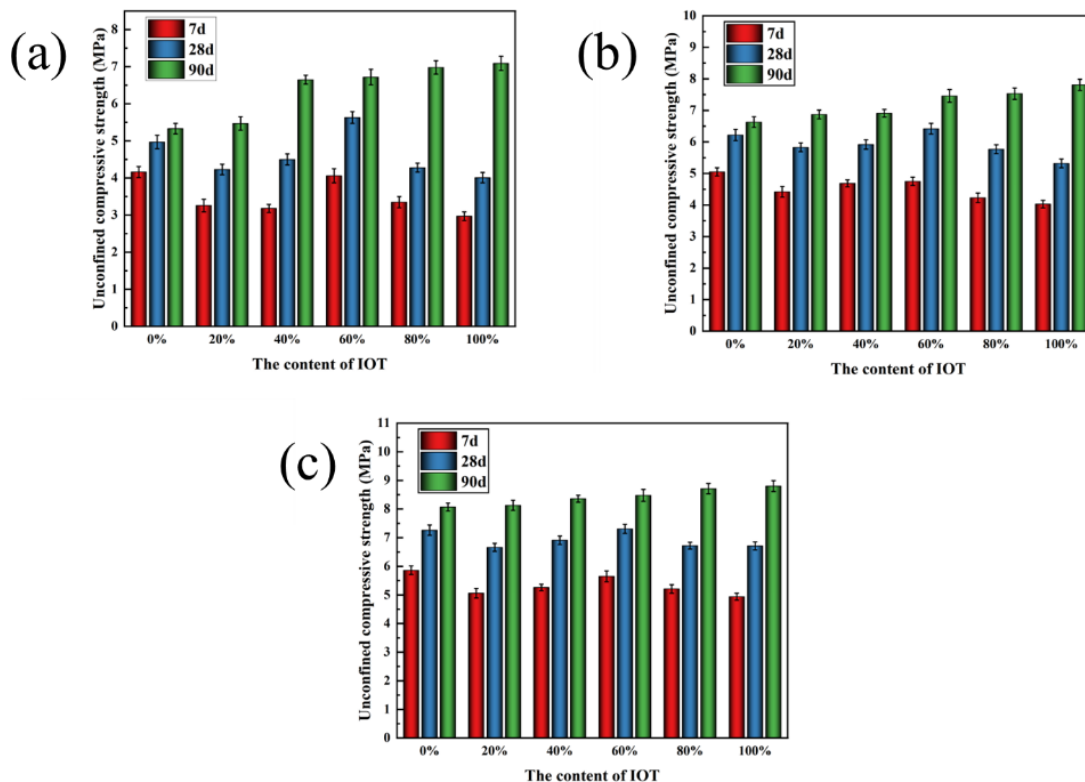


Fig. 5. Unconfined compressive strength of cement stabilized macadam for IOT.

strength of CSM with IOT replaced ratio of 100 % grew 73.08 % at the end of 28 d, and 17.78 % at 90 d. As comparison, the growth rate of CSM with 0 % IOT replacement ratio was only 7.89 %. with the cement dosage of 6 %, the splitting strength of CSM with 0 % IOT replacement ratio was 0.8 MPa at 90 d, while the split strength of CSM with a 100 % IOT replacement ratio was 0.89 MPa. This was because the active SiO₂ and Al₂O₃ in IOT reacted with the products of cement hydration to produce a gel material, which filled part of the pores and improved the deformation resistance of the specimen.⁴¹⁾ Finally, with the increase of

IOT content, the splitting strength of CSM gradually increased. The combined use of porous basalt coarse aggregates and IOT sand improved the splitting tensile strength of CSM due to their relatively rough surface increased the friction of interface.

Fig. 7 shows the longitudinal section of the fracturing strength experiment of CSM. The curing period is 90 d. The left picture shows the porous basalt CSM, and it can be seen that its section aggregate is broken seriously, the section surface is uneven, and the overall bonding strength of the CSM is low. The right picture shows the section diagram of

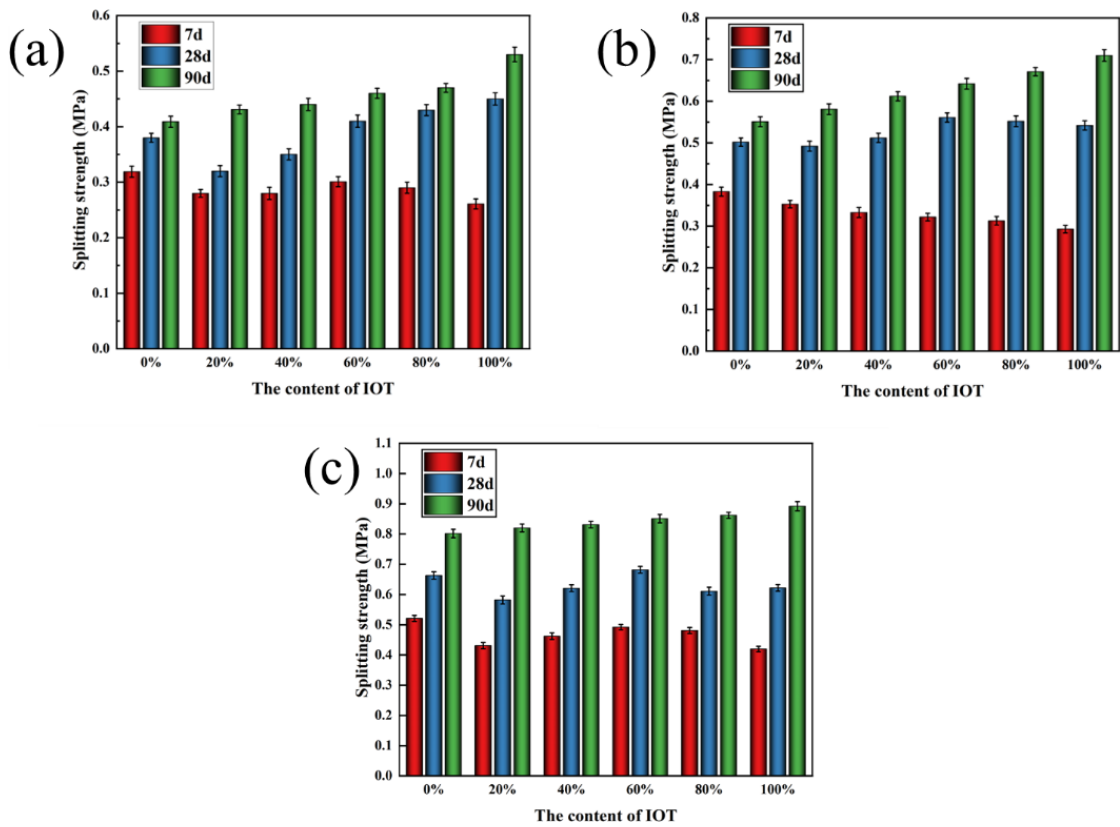


Fig. 6. Splitting strength of cement stabilized macadam for IOT.

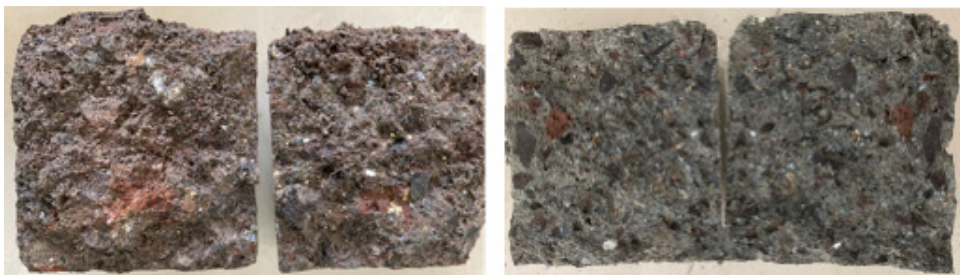


Fig. 7. Longitudinal section of the splitting test of cement stabilized macadam for IOT with 5 % cement content (left: 0 % IOT; right: 100 % IOT).

the specimen where 100 % iron tailings replace porous basalt fine aggregate with flat surface. The coarse aggregate without edge basically has no phenomenon of breaking and peeling, and the overall bond strength of CSM is higher.

3.3. Compressive rebound modulus

It can be seen from Fig. 8 is compressive rebound modulus of CSM-IOT with cement dosage of 4 %, 5 %, and 6 %, respectively. With the increase of cement dosage, the rebound modulus of CSM also increased gradually, and the rebound modulus reached the maximum when the cement was 6 %. As shown in Fig. 8(a), once the cement dosage was unchanged, the rebound modulus with IOT replacement ratio of 0 % was the largest at 7 d, while the rebound modulus with IOT replaced ratio of 100 % was the smallest. With the curing age of the specimens increased to 28 d, the growth rate of rebound modulus of the specimen with IOT replaced ratio of 0 % was 34.1 %, and that of specimen with IOT replaced ratio of 60 % was closed. However, with the increase of IOT replaced ratio, the compressive rebound modulus of CSM also increased with the increase use of IOT. The maximum compressive rebound modulus of 100 % IOT replaced ratio was 1,286 MPa, compared with the growth rate of 35.8 % for

28 d. When the cement dose was 6 % and the curing time reaches 90 d, the modulus of compressive rebound with 0 % IOT replaced ratio was 1,780 MPa, with a growth rate of 16.34 %, while the growth rate of samples with 100 % IOT replacement ratio was 27.15 %. This indicated that adding a certain amount of IOT could improve the modulus of compressive rebound of CSM in the later stage.

3.4. Freeze-thaw cycle

From Fig. 9 is variation value of freeze-thaw strength CSM-IOT with a cement dose of 4 %, 5 %, and 6 %, respectively. With the increase of cement dosage, the freeze-thaw resistance of cement-stabilized crushed stone material became stronger. When the cement dosage was 4 %, the 28 d unconfined compressive strength of cement-stabilized crushed stone material first increased and then decreased with the increase of IOT content. At 60 %, the peak value was 5.67 MPa, and the 28 d freeze-thaw cycle loss was also the same change. When the IOT replacement ratio was 0 %, the freeze-thaw splitting strength loss ratio of CSM was 87.8 %, and when the IOT replacement ratio was 100 %, the freeze-thaw splitting strength loss ratio was 82.1 %, indicated that adding too much IOT led to the deterioration of the

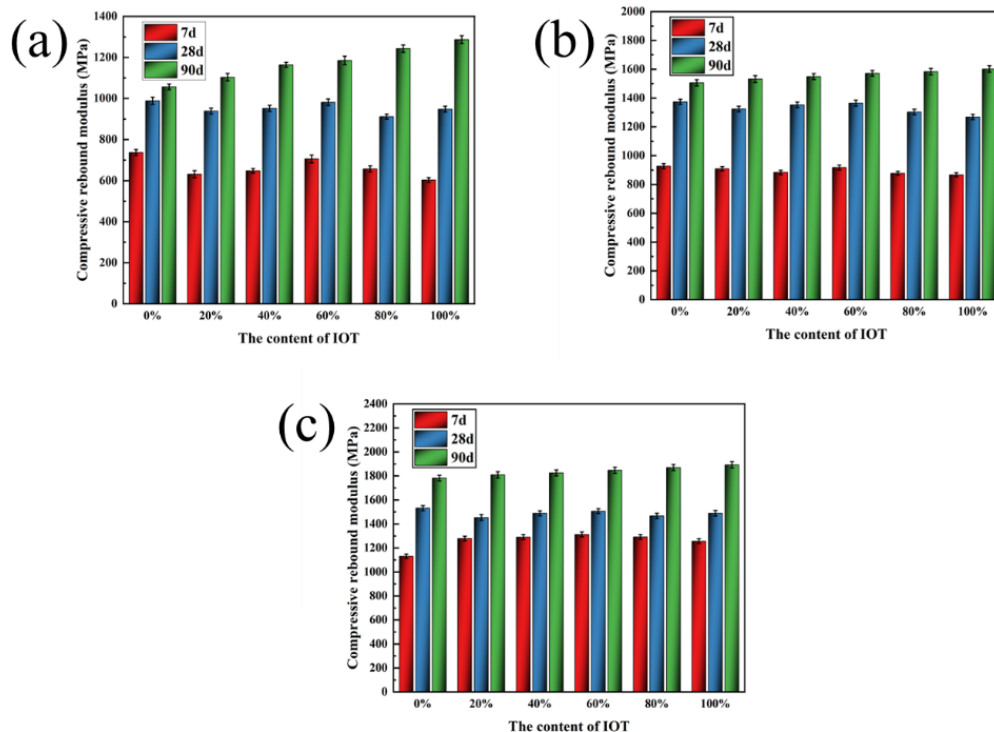


Fig. 8. Compressive rebound modulus of cement stabilized macadam for IOT.

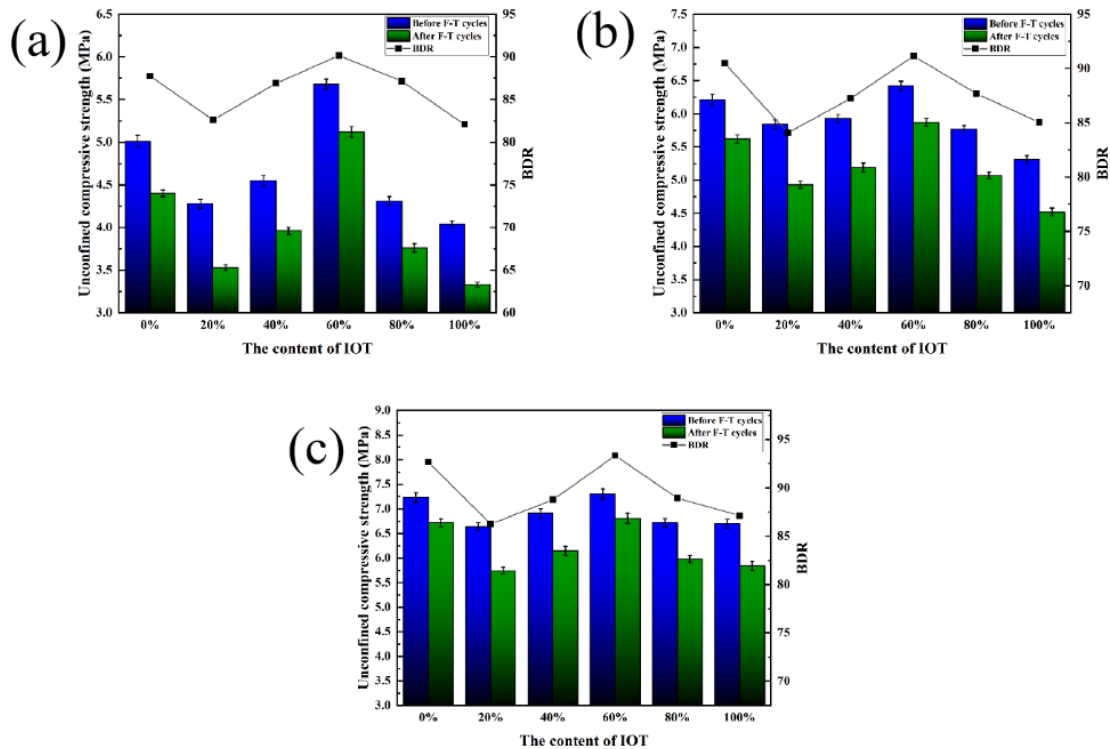


Fig. 9. Variation value of freeze-thaw strength of cement stabilized macadam for IOT.

freeze-thaw resistance of CSM. When the cement dosage was 6 %, the BDR of the control group was 92.7 %, the BDR of freeze-thaw split strength with 60 % IOT replacement ratio was 93.4 %, and the BDR of 100 % IOT replacement ratio was 87.3 %. The overall effect was good, indicating that a certain amount of IOT can improve the freeze-thaw resistance of CSM.⁴²⁾

3.5. EDTA titration method

Fig. 10 shows the CSM with 6 % cement dosage. The change value of Ca²⁺ content under different ages and different IOT dosage was measured. As shown in Fig. 10, at 7 d, the consumption of EDTA-2Na standard solution also increased with the increase of IOT content, indicating that the content of Ca²⁺ increased with the increase of IOT content. The dosage of cement was fixed, so the Ca²⁺ provided by cement were the same for CSM with different IOT contents. In the early stage of curing, the volcanic ash reaction rate of IOT and the components in cement was slow. There were slightly dissolved calcium salts in IOT, so the Ca²⁺ provided by the slightly dissolved calcium salts in IOT dominated the early mixture. Therefore, in the early stage, Ca²⁺ in the solution increased with the increase of IOT content.

At 28 d, the content of Ca²⁺ in the mixed solution with IOT content of 0 % was the highest. With increasing IOT content (20 %, 40 %, 60 %), SiO₂ and Al₂O₃ in IOT react with Ca²⁺ from cement hydration by pozzolanic effect and consume calcium hydroxide, so the graph reacts as a gradual decrease in Ca²⁺ content. At 60 %, the Ca²⁺ content in the mix is the lowest, which shows that the Ca²⁺ from cement hydration

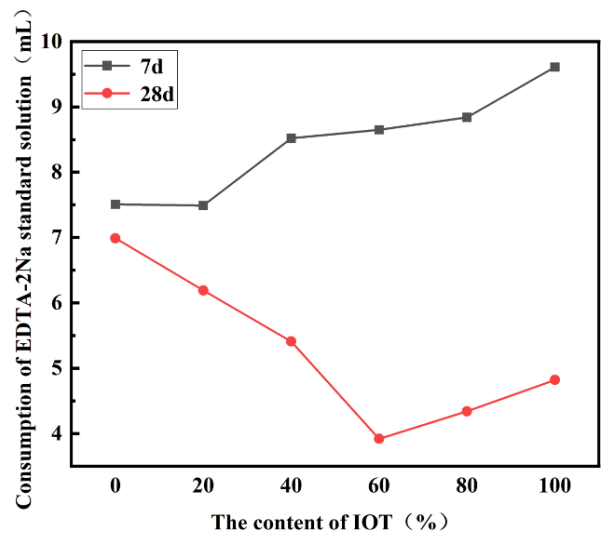


Fig. 10. Standard solution consumption of EDTA-2Na with different replacement percentage of IOT.

reacts with SiO_2 and Al_2O_3 in the IOT to reach the optimum value. However, there is a small amount of dissolved calcium salts in the IOT, so when the IOT content is (80 %, 100 %), a large amount of IOT will continue to dissolve Ca^{2+} , causing a gradual increase in the Ca^{2+} content of the solution. Therefore, in the later stage, silica in IOT reacted with

calcium hydroxide generated by cement hydration, which had a certain impact on the performance of CSM.⁴³⁾

3.6. Microstructure analysis of CSM

As can be seen from Fig. 11, reaction products with different morphologies can be found, and the morphologies

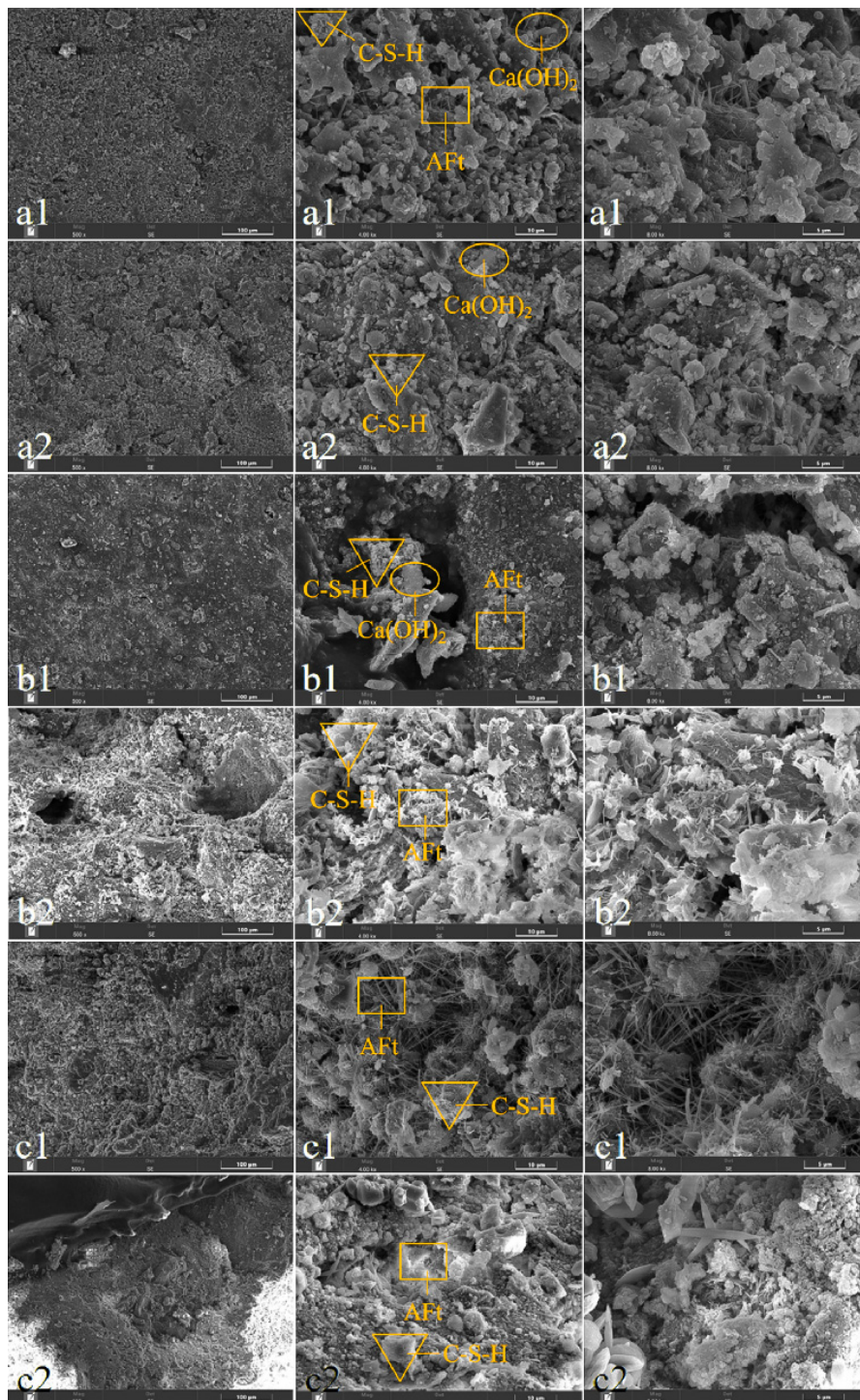


Fig. 11. Microstructure analysis diagram for cement stabilization of IOT.

of the products, such as C-S-H gel, Aft and $\text{Ca}(\text{OH})_2$, were determined by comparative analysis.⁴⁴⁻⁴⁶⁾ a1 is the CSM 7 d micromorphology with IOT replacement ratio of 0 %, and a2 is the CSM 7 d micromorphology with IOT replacement rate of 100 %. When the curing age of CSM was 7 d, it can be seen from a1 that the surface of CSM was relatively smooth and dense, with more C-S-H gel generated. Less Aft and $\text{Ca}(\text{OH})_2$ were generated, while a2 found that CSM with a 100 % IOT replacement ratio had partial pores on its surface, which was not as dense as CSM with a 0 % IOT replacement ratio. It also had partial C-S-H gel and $\text{Ca}(\text{OH})_2$. This indicated that CSM with 0 % IOT replacement ratio in the early days was more dense than CSM with 100 percent IOT replacement ratio. When CSM was maintained for 28 d, b1 is the CSM 28 d microtopography with 0 % IOT replacement ratio, and b2 was the 28 d microtopography with 100 % IOT replacement rate. It can be found that there was more Aft in b2, indicated that in CSM with 100 % IOT replacement rate, the cement and SiO_2 and Al_2O_3 in IOT had pozzolanic effect to generate more hydration products, which made the slurry surface denser. When CSM was cured for 90 d, c1 is the CSM 90 d microstructure map with 0 % IOT replacement rate, and c2 is the 90 d microstructure map with 100 % IOT replacement rate. It can be seen that both CSM with 0 % IOT replaced ratio and CSM with 100 % IOT replaced ratio have a large number of hydration products generated. With the increase of curing age, the CSM will become more and more dense and the internal hydration products will be more and more.

4. Conclusion

This paper mainly studies the application of IOT replacing porous basalt in pavement base, and studies the mechanical properties and durability of IOT cement-stabilized gravel materials prepared with different IOT replacement rates. The conclusions are as follows:

- (1) From the micro-morphology of IOT, it can be seen that it was angular, rough. With the curing age of 7 d and cement dosage of 4 %, the CSM of IOT with a replaced ratio of 0 % and 60 % met the basic requirements of highway grade heavy traffic highways and first-class highways. With IOT replacement rates of 20 %, 40 %, 80 %, and 100 %, CSM can meet the requirements of

highways with medium to light traffic and first-class highways.

- (2) With increasing cement dosage, the unconfined compressive strength, splitting strength and compressive resilient modulus of IOT cement stabilized macadam gradually increased. When the cement dosage is fixed, at ages of 7 d and 28 d, the incorporation of IOT leads to a decrease in the properties of CSM such as unconfined compressive strength, splitting strength, and compression resilience modulus. When the age is increased to 90 d, the various mechanical properties of CSM increase with the increase of IOT replacement rate.
- (3) When the cement dose was 6 %, and the curing age was 7 d. With the increase of IOT content, the content of Ca^{2+} increased with the increase of IOT content. When the curing age was 28 d, the content of Ca^{2+} decreased first and then increased with the increase of IOT content. At the age of 28 d, more C-S-H gel and Aft can be seen generated by IOT cement-stabilized gravel material, indicating that the active substances in IOT will have volcanic ash effect with the components in the cement.

Acknowledgement

This work was financially supported by The University Synergy Innovation Program of Anhui Province (GXXT-2022-083, GXXT-2023-019), Academic Funding Program for top discipline (major) talents in universities (No. gxbjZD 2022029), Major Science and Technology Project of Anhui Province (No. 202203c08020001), Excellent Scientific Research and Innovation Team in Colleges and Universities of Anhui Province (2022AH010017), and Anhui Province 15th batch "115" industrial innovation team.

References

1. P. H. Wen, C. H. Wang, L. Song, L. L. Niu and H. Y. Chen, *Sustainability*, **13**, 11610 (2021).
2. T. Meng, S. S. Lian, K. J. Ying and H. M. Yu, *Rev. Adv. Mater. Sci.*, **60**, 490 (2021).
3. C. Berthelot, D. Podborochynski, B. Marjerison and T. Saarenketo, *Can. J. Civ. Eng.*, **37**, 1613 (2010).
4. A. J. Puppala, S. Saride and R. Williammee, *J. Mater. Civ. Eng.*, **24**, 418 (2012).

5. G. P. Qian, T. Huang and S. Y. Bai, *J. Mater. Civ. Eng.*, **23**, 1575 (2011).
6. W. Tabyang, C. Suksiripattanapong, C. Phetchuay, C. Laksanakit and N. Chusilp, *Road Mater. Pavement Des.*, **23**, 2178 (2021).
7. S. W. Townsend, C. J. Spreadbury, S. J. Laux, C. C. Ferraro, P. E. R. Kari and T. G. Townsend, *J. Environ. Eng.*, **146**, 0402 (2020).
8. S. H. Liang, J. T. Chen, M. X. Guo, D. L. Feng, L. Liu and T. Qi, *Waste Manage.*, **105**, 425 (2020).
9. L. A. Guerrero, G. Maas and W. Hogland, *Waste Manage.*, **33**, 220 (2013).
10. O. R. Carmignano, S. S. Vieira, A. P. C. Teixeira, F. S. Lameiras, P. R. G. Brandao and R. M. Lago, *J. Braz. Chem. Soc.*, **32**, 1895 (2021).
11. J. S. Zhao, K. Ni, Y. P. Su and Y. X. Shi, *Constr. Build. Mater.*, **286**, 122968 (2021).
12. B. C. Gayana and K. R. Chandar, *Adv. Concr. Constr.*, **6**, 221 (2018).
13. J. H. Deng, X. A. Ning, J. H. Shen, W. X. Ou, J. Y. Chen, G. Q. Qiu, Y. Wang and Y. He, *J. Environ. Manage.*, **317**, 115435 (2022).
14. N. Zhang, B. W. Tang and X. M. Liu, *Constr. Build. Mater.*, **288**, 123022 (2021).
15. C. Li, H. H. Sun, Z. L. Yi and L. T. Li, *J. Hazard. Mater.*, **174**, 78 (2010).
16. J. L. B. Galvao, H. D. Andrade, G. J. Brigolini, R. A. F. Peixoto and J. C. Mendes, *J. Cleaner Prod.*, **200**, 412 (2018).
17. Y. Liu, W. R. Hao, W. He, X. Meng, Y. L. Shen, T. Du and H. Wang, *Coatings*, **12**, 95 (2022).
18. C. Li, N. Zhang, J. C. Zhang, S. Song and Y. H. Zhang, *Materials*, **15**, 112 (2021).
19. J. S. Zhao, Y. P. Su, Y. X. Shi, Q. X. Wang and K. Ni, *Struct. Concr.*, **23**, 423 (2022).
20. F. H. Han, S. M. Song, J. H. Liu and S. Huang, *Powder Technol.*, **345**, 292 (2019).
21. B. G. Ma, L. X. Cai, X. G. Li and S. W. Jian, *J. Cleaner Prod.*, **127**, 162 (2016).
22. W. C. Fontes, J. C. Mendes, S. N. Da Silva and R. A. F. Peixoto, *Constr. Build. Mater.*, **112**, 988 (2016).
23. L. X. Cai, B. G. Ma, X. G. Li, Y. Lv, Z. L. Liu and S. W. Jian, *Constr. Build. Mater.*, **128**, 361 (2016).
24. N. Garcia-Troncoso, H. Baykara, M. H. Cornejo, A. Riofrio, M. Tinoco-Hidalgo and J. Flores-Rada, *Case Stud. Constr. Mater.*, **16**, e01031 (2022).
25. M. J. Yang, J. H. Sun, C. Y. Dun, Y. J. Duan and Z. L. Meng, *Constr. Build. Mater.*, **265**, 120760 (2020).
26. S. Abd Latif, M. S. A. Rahman and O. Sikiru, *Rom. J. Mater.*, **47**, 336 (2017).
27. S. Zhao, J. Fan and W. Sun, *Constr. Build. Mater.*, **50**, 540 (2014).
28. W. Li, L. Lang, Z. Y. Lin, Z. H. Wang and F. G. Zhang, *Constr. Build. Mater.*, **134**, 540 (2017).
29. J. A. Wang, A. C. Fayish, B. Hoffheins and M. L. McCahan, *Transp. Geotech.*, **30**, 100618 (2021).
30. A. H. Farhan, A. R. Dawson and N. H. Thom, *Mater. Des.*, **97**, 98 (2016).
31. D. Singh and A. Kumar, *J. Rock Mech. Geotech. Eng.*, **9**, 370 (2017).
32. Y. X. Li, S. B. Ma, G. Chen and S. Wang, *Int. J. Pavement Eng.*, **24**, 2011278 (2021).
33. J. Zhang, C. Li, L. Ding and J. Li, *Constr. Build. Mater.*, **296**, 123596 (2021).
34. X. Lan, X. Zhang, Z. Hao and Y. Wang, *Case Stud. Constr. Mater.*, **16**, e00984 (2022).
35. K. Yan, G. Li, L. You, Y. Zhou and S. Wu, *Constr. Build. Mater.*, **233**, 117326 (2020).
36. K. Yan, H. Sun, F. Gao, D. Ge and L. You, *J. Cleaner Prod.*, **244**, 118750 (2020).
37. C. F. Chu, Y. F. Deng, A. N. Zhou, Q. Feng, H. Ye and F. S. Zha, *Constr. Build. Mater.*, **189**, 849 (2018).
38. L. A. D. Bastos, G. C. Silva, J. C. Mendes and R. A. F. Peixoto, *J. Mater. Civ. Eng.*, **28**, 04016102 (2016).
39. Ministry of Transport PR China. Test methods of materials stabilized with inorganic binders for highway engineering (JTG.E51-2009). Retrieved October 15, 2009 from https://xxgk.mot.gov.cn/2020/jigou/glj/202403/t20240301_4032012.html
40. Ministry of Transport PR China. Technical guidelines for construction of highway roadbases (JTG/T.F20-2015). Retrieved July 30, 2015 from https://xxgk.mot.gov.cn/2020/jigou/glj/202006/t20200623_3312274.html
41. Y. Cheng, F. Huang, W. Li, R. Liu, G. Li and J. Wei, *Constr. Build. Mater.*, **118**, 164 (2016).
42. J. Han, C. Fu, S. Liu, H. Li, L. Wang, H. Sun, H. Wu and A. Gloria, *Adv. Mater. Sci. Eng.*, **2022**, 8028009 (2022).
43. R. Wu, Y. Zhang, G. Zhang and S. An, *J. Build. Eng.*, **57**, 104954 (2022).
44. M. Gao, J. Dai, H. Jing, W. Ye and T. Sesay, *J. Build. Eng.*, **403**, 133065 (2023).
45. B. Liu, H. Meng, G. Pan and D. Li, *Adv. Cem. Res.*, **35**, 258 (2022).
46. J. Liu, S. An and Y. Zhang, *Cem. Concr. Compos.*, **140**, 105061 (2023).

Author Information

Qifang Ren

Associate Professor, School of Materials Science and Chemical Engineering, Anhui Jianzhu University

Fan Bu

Researcher, School of Materials Science and Chemical Engineering, Anhui Jianzhu University

Qinglin Huang

Researcher, School of Materials Science and Chemical Engineering, Anhui Jianzhu University

Haijun Yin

Researcher, Beijing Rechsand Sand Industry Casting Material Co., Ltd.

Yuelei Zhu

Researcher, School of Materials Science and Chemical Engineering, Anhui Jianzhu University

Rui Ma

Lecturer, School of Materials Science and Chemical Engineering, Anhui Jianzhu University

Yi Ding

Professor, School of Materials Science and Chemical Engineering, Anhui Jianzhu University

Libing Zhang

Researcher, Anhui Road and Bridge Engineering Group Co., Ltd.

Jingchun Li

Researcher, Anhui Road and Bridge Engineering Group Co., Ltd.

Lin Ju

Researcher, Anhui Road and Bridge Engineering Group Co., Ltd.

Yanyan Wang

Researcher, Anhui Institute of Building Research and Design

Wei Xu

Researcher, Anhui Construction & Building Materials Technology Group Co., Ltd.

Haixia Ji

Researcher, School of Materials Science and Chemical Engineering, Anhui Jianzhu University

Won-Chun Oh

Professor, Department of Advanced Materials Science and Engineering, Hanseo University